A POST IMPACT VOLCANISM SCENARIO FOR THE FORMATION OF THE OLIVINE-RICH UNIT IN THE REGION OF NILI FOSSAE, MARS.

L. Mandon[1], C. Quantin[1], P. Thollot[1], L. Lozac'h[1], N. Mangold[2], G. Dromart[1], P. Beck[3], E. Dehouck[1], S. Breton[1], C. Millot[1].
[1] Laboratoire de Géologie de Lyon Terre, Planètes, Environnement, Université de Lyon, France. [2] Laboratoire de Planétologie et Géodynamique, Université de Nantes, France. [3] Institut de Planétologie et d'Astrophysique de Grenoble, Université Grenoble Alpes, France. lucia.mandon@univ-lyon1.fr.

Introduction: The Nili Fossae region exhibits the largest Martian exposures of olivine-rich materials, as deduced from orbital near-infrared and thermal spectroscopy [1, 2]. Several hypotheses have been proposed to explain the origin of a widespread olivine-rich formation in the region: (1) these materials might be crustal rocks excavated by the giant impact leading to the formation of Isidis Planitia [2], a 1200 km wide impact basin east of Nili Fossae. (2) They could result from mafic effusive lava flows occurring before [3] or after [4] the giant impact. (3) The unit itself could be the remnants of an impact melt sheet rich in olivine and resulting from the Isidis impact [5]. The bandings observed in the olivine-rich unit are in conflict with an intrusive origin, yet it is not clear whether the unit results from an impact melt sheet or from eruptive flow. Here, we analyze high-resolution data to study the stratigraphic contacts of this unit and its geometry. We also perform crater size distribution measurements to infer the exposure time of the unit to bombardment. A more precise understanding and timing of the geological history in the region of Nili Fossae would give more apprehension of two landing sites proposed for the Mars2020 rover mission (NASA), Jezero crater and Northeast Syrtis, as this unit is exposed in both sites.

Data and methods: The mapping of the olivine-rich unit of the region has been achieved based on the diagnostic absorption feature of olivine, centered near 1 µm. We processed data from the imaging spectrometers OMEGA (Observatoire pour la Minéralogie, l'Eau les Glaces et l'Activité) onboard Mars Express Mission and CRISM (Compact Reconnaissance Imaging Spectrometer for Mars) onboard Mars Reconnaissance Orbiter using the MarsSI web application [6]. Spectral data are calibrated to I/F reflectance and corrected from atmospheric contribution. Spectral parameters for olivine and Fe/Mg phyllosilicates were calculated and mapped at scales of 350 m/pixel up to 5 km/pixel (OMEGA data) and 200 m/pixel (CRISM survey data); combination of both enables regional to local interpretation of the mineralogy and good coverage of the area. To infer the stratigraphic contacts as well as the morphology of the unit, we processed visible images from the CTX (Context Camera) and the HiRISE (High Resolution Imaging Science Experiment) cameras onboard Mars Reconnaissance Orbiter. We also computed HiRISE DTMs from stereopairs of science targets using MarsSI. We used HRSC DTMs computed by the Freie Universitaet Berlin and DLR Berlin. Strikes and dips measurements were performed using the ArcGIS extension LayerTools [7]. Finally, we performed crater size analyses on both small (~1 km²) and wide (~900 km²) olivine-rich areas. Using the Craterstats software [8], we compared size distributions to isochrons generated by the Ivanov production function to estimate a surface age [9].

Results: At HiRISE resolution, the unit appears light-toned and exhibits polygonal fracturing. It lies above the regional Fe/Mg phyllosilicates altered basement and is overlain by a capping unit with muted spectral signatures [10]. At some locations in the northern part of the region, the olivine-rich bedrock displays tens of meters thick bands (Fig. 1) and is often found filling depressions within the altered basement. In addition, the olivine-poor capping unit is restricted to depressions in the topography and appears to have filled the lowest parts of the region. In the Northern parts of the Noachian crater Jezero, where the rim is highly-eroded, the olivine-rich unit overlaps the topography and appears to fill the floor of the crater (Fig. 2). Preliminary results from strike and dip measurements on the olivine-rich unit bandings indicate relatively low dips, ranging from 1 to 9°, with strikes often oriented parallel to the contact (Fig. 3).

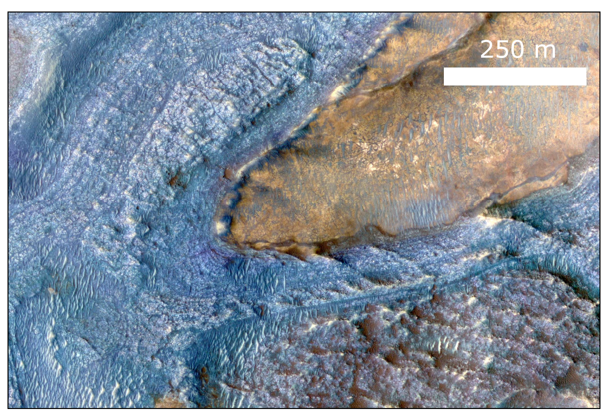

Figure 1. Color-enhanced HiRISE PSP_006712_2020 (region of Nili Fossae). The banded olivine-rich, altered phyllosilicates basement and capping unit appears respectively blue, orange and dark purple.

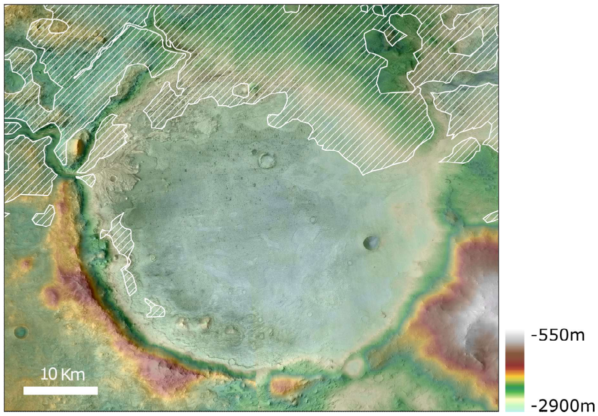

Figure 2. Map of exposed olivine-rich materials (white) based on spectral data and morphology observation over Jezero crater. HRSC elevation is overlain on a CTX mosaic.

Differential size frequency distribution of craters smaller than 200 m shows saturation of the surface. Yet craters larger than 1 km distribution aligns on Noachian ages, with a minimum surface age of ~3.8 Ga. The distribution also exhibits a strong depletion in small craters, implying that the olivine-rich unit has been widely subject to obliteration over time.

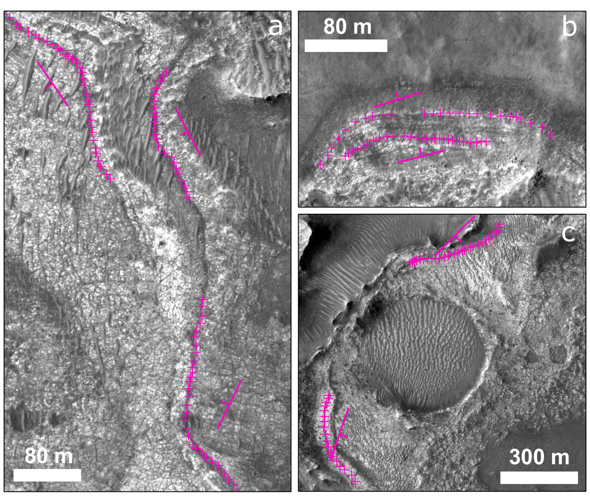

Figure 3. Views of (a, b) HiRISE ESP_044095_2010 and (c) ESP_045005_2010 showing geometries of olivine-bearing layers (bright outcrops) along measurement points (region of Nili Fossae).

Formation scenarios: Timing for the formation of the olivine-rich unit of the Nili Fossae region is constrained by stratigraphic relationships: (1) the olivine-rich unit overlaps the northern parts of the rim of Jezero crater, dating its emplacement after the formation and erosion of the crater. The highest part of the rim reaches an elevation of ~-1500 m and the eroded parts ~-2300 m. Given a maximum Noachian rim erosion rate of 10 m/Ma [11], we can estimate on the order of at least ~tens of Ma between the formation of Jezero crater and the emplacement of the olivine-rich unit in the crater. (2) Jezero crater is located on the inner rim of Isidis basin. It is very unlikely that it formed before Isidis, as the preservation state and steep scarp of the southwest part of Jezero rim are not consistent with burial below thick impact melts and ejecta. The above leads to the conclusion that there is a gap of millions of years between the impact of Isidis and the emplacement of the latest olivine-rich exposures; this is inconsistent with the pre-Isidis and impact melt scenarios. The Isidis impact has been dated at 3.96 Ga [12]: taking in account the time for Jezero rim erosion and results from crater counts, this yields a formation age of ~3.8–3.9 Ga for the olivine-rich unit. Given the stratigraphic and morphologic evidence, there is no argument to reject the scenario of a post-impact volcanism origin. The thinnest crust on Mars has been inferred beneath Isidis basin [13]. In a context of impact-fragilized and thinned crust, magma would have propagated through the fractures to form dykes and easily reached the surface similarly to lunar mare-volcanism, supporting the hypothesis of Tornabene et al. [4]. In comparison to what is observed in the region, volcanism post-dating by hundreds of millions of years a giant impact is also seen on Mars associated to the Hellas basin [14].

Conclusion: Based on stratigraphic evidence and crater counts, we estimate the age of the Nili Fossae regional olivine-rich unit to be comprised between ~3.8 and ~3.9 Ga (mid–late Noachian). We favor the hypothesis of a post-Isidis volcanism origin, that would have been facilitated by a thinned and fractured crust context following the giant impact.

References: [1] Mustard J. F. et al. (2005) *Science*, *307*, 1594–1597. [2] Hoefen T. M. et al. (2003) *Science*, *302*, 627–629. [3] Hamilton V. E. and Christensen P. R. (2005) *Geology*, *33(6)*, 433–436. [4] Tornabene L. L. et al. (2008) *JGR*, *113(E10)*. [5] Mustard J. F. et al. (2007) *JGR*, *112(E08)*. [6] Quantin-Nataf C. et *al.* (2017) *in press to PSS*. [7] Kneissl T. et *al.* (2010) LPS XLI, Abstract #1640. [8] Michael G. G. and Neukum G (2010) *Earth Planet. Sci. Lett.*, *294(3-4)*, 223–229. [9] Ivanov B. A. (2001) *Space Sci. Rev.*, *96*, 87-104. [10] Mustard J. F. et al. (2009) *JGR*, *114(E00)*. [11] Craddock R. A. and Maxwell T. A. (1993) *JGR*, *98(E2)*, 3453–3468. [12] Werner S. C. (2008) *Icarus*, *195(1)*, 45–60. [13] Zuber M. T. et al. (2000) *Science*, *287*, 1788–1793. [14] Williams D. A. et al. (2009) *PSS*, *57*, 895–916.